Synthesis of Octachloro- and Octaazido-Functionalized T 8 -Cages and Application to Recyclable Palladium Catalyst

Yujia Liu, Kyoka Koizumi, Nobuhiro Takeda, Masafumi Unno, Armelle Ouali

Synthesis of octachloro and octaazido-functionalized T_8 cages and application to recyclable palladium catalyst

Yujia Liu,[a] Kyoka Koizumi,[b] Nobuhiro Takeda,[b] Masafumi Unno,[a,b] Armelle Ouali*[a,c]*

a. Gunma University Initiative for Advanced Research (GIAR)-International Open Laboratory with ICGM France

b. Department of Chemistry and Chemical Biology, Graduate School of Science and Technology. Gunma University, Kiryu 376-8515, Japan

c. ICGM, Univ Montpellier, CNRS, ENSCM, Montpellier 34296, France.

ABSTRACT

Unprecedented T_8 cages bearing eight chloromethyldimethylsilylethyl substituents were obtained in excellent yield from the readily and commercially available octavinylsilsesquioxane. The chloro groups can be quantitatively substituted by azido ones to yield the corresponding octaazido T_8 without rearrangement of the cage. The syntheses of both functionalizable POSSs are scalable (gram-scale). The azido-functionalized T_8 compound constitutes a versatile building block able to undergo copper-catalyzed azide-alkyne [3+2] cycloaddition. As a proof of concept, it was allowed to react with 2-ethynylpyridine to give rise to a multidentate ligand bearing eight 2-pyridyl-triazole moieties (*N,N*-pincers). The coordination of the eight *N,N*-bidentate ligands to palladium (II) led to the corresponding octa-palladium complex shown to successfully promote the cross-coupling reaction between anisole and phenylboronic acid. The low solubility of this catalytic complex in the reaction medium enabled (or facilitated or made possible) its straightforward recovery and recycling with four cycles with no loss of activity.

Introduction

Hybrid nanostructured molecules that combine the advantages of the inorganics and organics at the molecular level attract growing interest for designing high performance materials. Along these lines, polyhedral oligomeric silsesquioxanes (POSS), involving inorganic thermostable Si-O-Si core decorated with organic reactive peripheral flexible moieties, appear as appealing candidates.[1] In particular, the cubic octasilsesquioxanes (T_8) have been intensively studied due to their unique properties[2,3] and they constitute a versatile and tunable platform finding applications in various fields such as catalysis,[4] sensors,[5] membranes,[6] photoactive materials[7] or biomass-based nanocomposites[8] to name a few. The search for fast and scalable routes to functionalizable T_8-cages is still a very active research field.

Among functionalizable T_8-cages, those decorated with azido functions are considered as precursors with high potential to design multifunctional materials. Indeed, the azido moieties are able to react with a wide array of alkynes through copper-catalyzed Huisgen [3+2] cycloaddition (CuAAC).[9] This efficient chemical transformation, attractive in terms of atom-economy, enabling expedited synthetic processes with quantitative yields and short reaction times is recognized as a "click reaction". In addition, the chemical robustness of the generated triazole linkage also constitutes an asset of this ligation method currently widely used to functionalize molecules or nano-sized objects and access functional materials. Hence azido-containing POSSs with several inorganic frameworks have been previously reported. For example, we,[10] and other groups[11] reported double-decker silsesquioxanes (DDSQs) bearing four or two azido end groups on their side chains respectively. In all cases, the DDSQs were obtained from their chloro counterparts in the presence of sodium azide. Besides DDSQs, most examples involve T_8 bearing one[12] or eight[13] azido terminal functions connected to the inorganic core through aliphatic or benzylic spacers. These cubic silsesquioxanes were functionalized via the CuAAC strategy to access hybrid polymeric materials,[12a-g,13a-j] recyclable catalysts,[12h-j] bio-active compounds[13k-o] or optoelectronic devices.[13p-q] The widely used octa(3-azidopropylsilsesquioxane) T_8 (T_8-propyl-N_3) can be prepared from the commercial acidic salt of the octa(3-aminopropylsilsesquioxane) (T_8-propyl-NH_2·HCl) and nonaflyl azide using diazo-transfer reactions.[14] This route suffers from fair yields (67%) and safety issues since diazo reagents are highly energetic molecules. A much preferred pathway consists in synthesizing the T_8-propyl-N_3 from the corresponding octa(3-chloropropylsilsesquioxane) (T_8-propyl-Cl) by nucleophilic substitution of the chlorides by azides.[11a,13b,k] However the latter reaction is very slow and nucleophilic-induced cage rearrangement occurs as shown by Kawakami, Ervithayasuporn et al. who reported the formation

of T_{10} and T_{12} cages together with the expected T_8 cage.[11a] The decaazido compound (T_{10} cage) was obtained as the major isomer after column chromatographies (~ 35% isolated yield) and was later on exploited as platform for developing applied materials.[12j,15] The yield of expected T_8-propyl-Cl can be improved by firstly converting the eight chlorides by better leaving groups such as bromides[13b] or iodides[13o]. In this work, a straightforward, selective and high-yielding synthetic route to octachloro and octaazido T_8 cages is described. These new compounds are obtained from readily prepared and commercially available octavinylsilsesquioxane **1** in very high yield and differ from the previously mentioned structures by the existence of a slightly longer arm between the edge of the inorganic core and the chloro or azido substituent (Scheme 1).

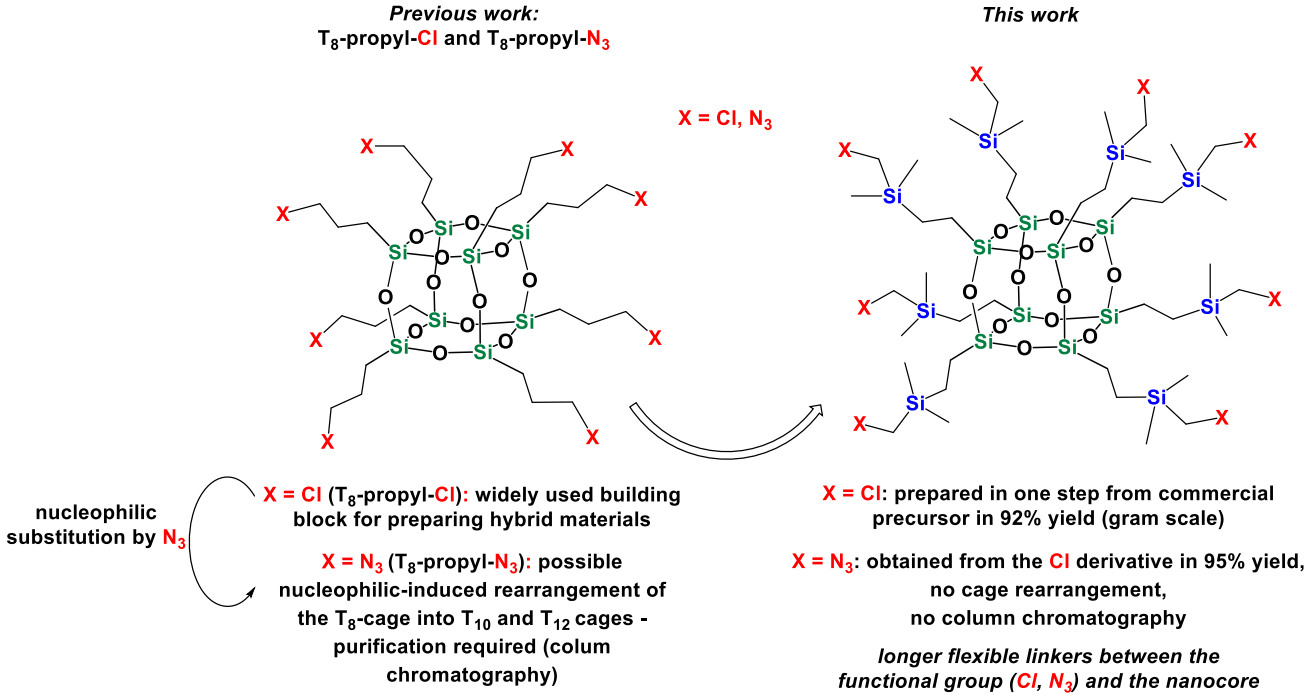

Scheme 1. Objective of the present work and comparison with previously reported T_8 cages decorated with eight chloropropyl or azidopropyl substituents.

The hydrosilylation of **1** with chloromethyldimethylsilane (**2**) was carried out in the presence of small amounts of Karstedt's catalyst (0.02 mol% of Pt / C=C bond) to afford **3** isolated in 92%

yield after filtration through a silica plug (Scheme 2). It is noteworthy that the hydrosilylation is completely regioselective to *β*-product. The nucleophilic substitution of the chlorides by azides was next performed in a THF/DMF (1:2.6) mixture and T_8 cage **4** could be isolated in 95% yield after extraction, without any further purification (Scheme 2). The addition of catalytic amounts of sodium iodide (12.5 mol % per Cl) was found to greatly accelerate the reaction. Both procedures enabling to prepare **3** and **4** can be achieved in gram scale (> 2.5 g for **3** and at least 740 mg for **4**, see experimental section).

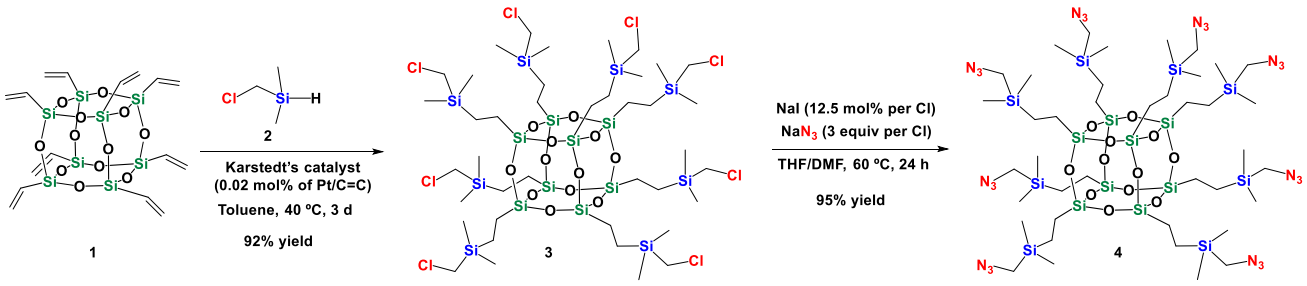

Scheme 2. Preparation of the octachloro T_8 cage **3** and octaazido T_8 cage **4**.

Compounds **3** and **4** were fully characterized by usual analytical techniques. The ^{29}Si NMR spectra displayed two singlets in each case (Figure 1, a and b respectively), the resonances at -66.49 ppm for **3** and -66.59 ppm for **4** being assigned to silicon atoms of the cage (Si in green) and the ones at 5.38 and 5.18 ppm corresponding to the carbosilanes (Si in blue). The latter chemical shifts were in the same range as those previously reported for related functionalized double-decker[10] and laddersiloxanes[16] and were also in accordance with the symmetrical structures of **3** and **4**. From the ^{13}C NMR spectra, **4** can be clearly distinguished from **3**, with about 10 ppm downfield shifted of the methylene protons between D-unit Si and azido group (Figure 1 d). ^{1}H NMR spectroscopy, elemental analysis and MALDI-TOF mass spectroscopy confirmed the structures of **3** and **4** as well, for example an experimental mass found at 1524.92 $g.mol^{-1}$ for **3** $[M+Na^+]$ that was in good accordance with the calculated one at 1525.15 $g.mol^{-1}$ (see experimental

section and Figures S1-S6, S14, S15). Moreover, in the case of **4**, the infrared spectrum highlighted the characteristic band corresponding to the azido group at 2098 cm^{-1} (Figures S18).

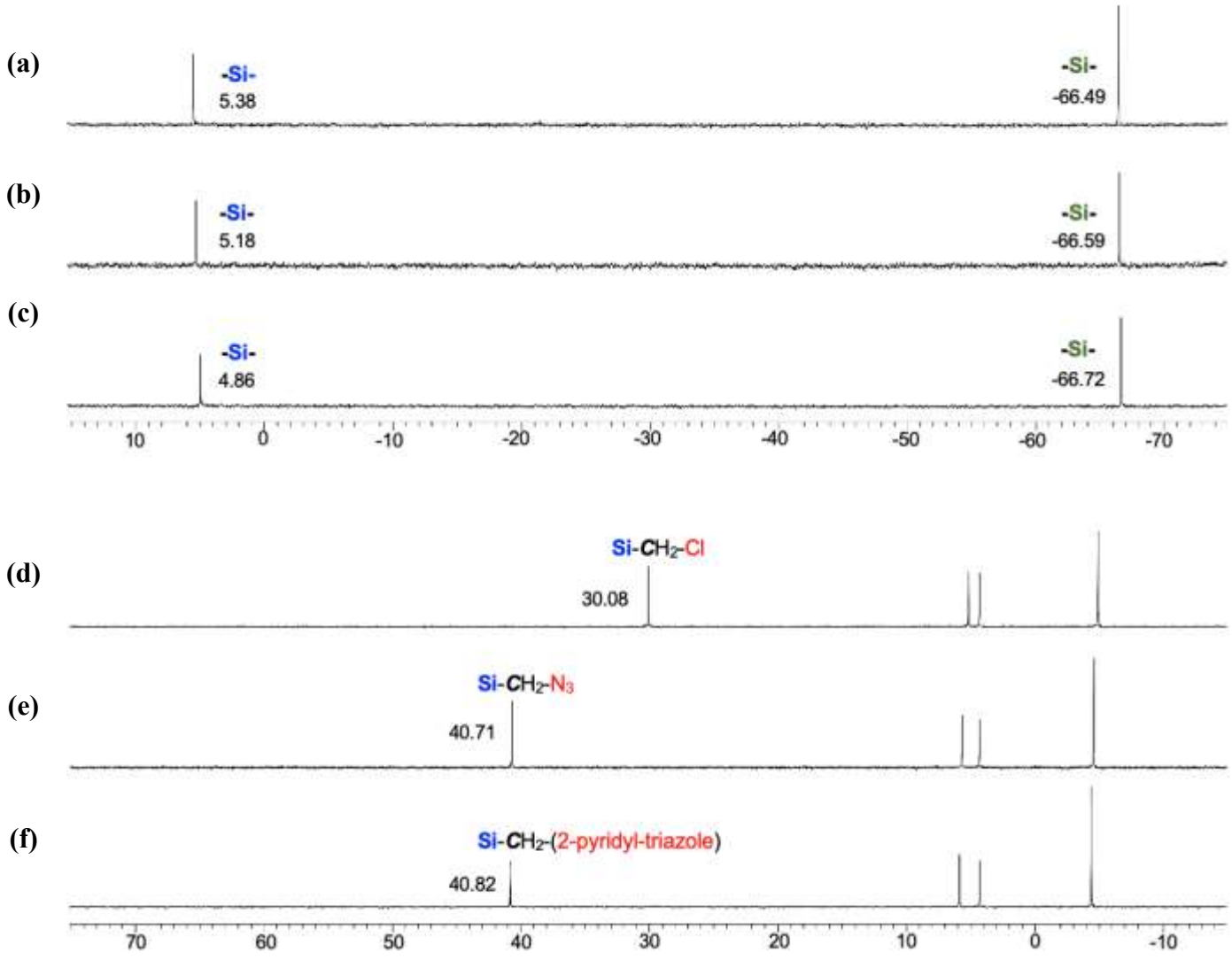

Figure 1. ^{29}Si NMR spectra (in $CDCl_3$) for the compounds **3**, **4** and **6** (**a, b** and **c** respectively) and and ^{13}C NMR spectra (in $CDCl_3$) for the compounds **3**, **4** and **6** (**d, e** and **f** respectively). Chemical shifts are in ppm unit.

Single crystals were grown and the structure of **4** could be determined by X-ray crystallography (Figure 3 and Table S1). To the best of our knowledge, the X-ray structure of the related T_8 cages bearing eight azido substituents has not been solved to date. For **4**, the Si-O bond lengths are found in the ranges of 1.612-1.635 Å (average 1.623Å) which corresponds to usual values reported for

T_8 cages and other siloxanes.[1c] The Si–O–Si bond angles vary from 140.6 to 158.4° (average 148.9°) which corresponds to a larger deviation as compared to the related octa(3-chloropropylsilsesquioxane) (T_8-propyl-Cl) 147.7 to 151.5° (average 149.8°).[1c] Such deviation (> 5 %) is encountered in T_8 cages decorated with chains containing 6 to 8 atoms (-$(CH_2)_2O(CH_2)_2Cl$; -$(CH_2)_2CMe_2CH_2CO_2Me$; n-oct for examples[1c]) and this is rationalized by the flexible structure of such frameworks.[1c] This is consistent with the presence of a longer carbosilane arm in the case of **4** compared to T_8-propyl-Cl.

The interatomic Si…Si distances were also measured and found in the range of 3.093-3.156 Å (average 3.121 Å) for the *o*-Si…Si, 4.384-4.452 Å (average 4.414 Å) for the *m*-Si…Si and 5.378-5.423 Å (average 5.406 Å) for the *p*-Si…Si. These average values are consistent with those reported for related T_8-cages (3.11-3.16 Å, 4.40-4.45 Å and 5.39-5.43 Å for the *o*-, *m*- and *p*-Si…Si respectively).[17]

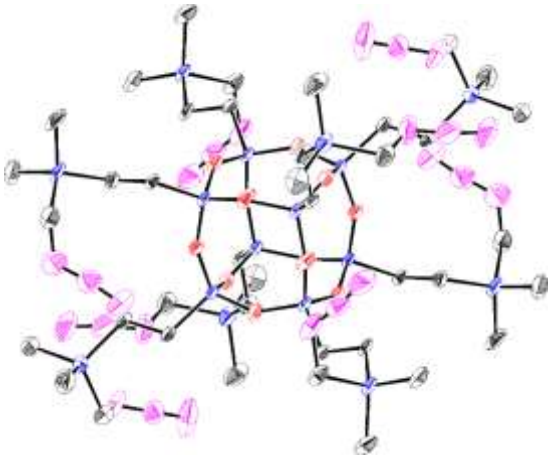

Figure 3. Crystal structure of **4**. Black: carbon; blue: silicon; red: oxygen; pink: nitrogen. Thermal ellipsoids are shown at the 50% probability level. All hydrogen atoms are omitted for clarity.

As expected, the results of the thermogravimetric analysis (TGA) under N_2 showed a lower Td_5 (158 °C, Table S2) for the azido-functionalized **4** compared to its tetrachloro counterpart **3** displaying a high thermal stability (Td_5 = 358 °C, Table S2). Both Td_5 are comparable to those of

related DDSQ frameworks bearing four azido (Td_5 = 167 °C) or four chloro (Td_5 = 359 °C) substituents.[11] As expected, the nature of the external substituents have more impact on the thermal stability of the decorated POSS than the structure of the intrinsically robust silsesquioxane nanocage itself.

As related octaazido cubic Si-O frameworks obtained from T_8-propyl-Cl[11a,13b,k] or derived from epoxy-hydroxyl-functionalized spherosilicates,[18,19] compound **4** reported here may be applied as a building block to design new hybrid nanostructures applicable in multiple areas.

Therefore, the reactivity of the external azido substituents was next evaluated as a proof of concept and **4** was allowed to react with 2-ethynylpyridine **5** through copper-catalyzed Huisgen [3+2] cycloaddition (CuAAC, Scheme 3). It is worthy to note that **5** is a highly challenging substrate that generally requires harsh temperature to be quantitatively functionalized.[20] In the case of **4**, the reaction proceeded selectively and quantitatively at room temperature for 3 days and the corresponding T_8 cage **6** decorated with eight peripheral 2-pyridinyl-triazole moieties could be isolated in 71% yield after column chromatography. Compound **6** was found to be soluble in common solvents including chloroform, THF, DMSO and its structure could be confirmed by multinuclear NMRs. The ^{29}Si NMR spectrum displayed two expected singlets (Figure 1c) respectively assigned to the silicon atoms from the core (Si in green, -66.72 ppm) and to the carbosilane-type silicon atoms (Si in blue, 4.86 ppm). Besides, the appearance of a singlet (^{1}H NMR) at 8.13 ppm in $CDCl_3$ and 8.38 ppm in DMSO-d_6, indicated the successful formation of the triazole ring (Figures S7 and S8).[20] The resonance of the methylene groups vicinal to the azide groups at 2.80 in **4** shifted to 3.99 ppm downfield in **6**, which is also consistent with the presence of the triazole moiety after click reaction (see Figure S7). Mass spectroscopy confirmed the structure as well (see experimental section and Figure S16). Remarkably, the 2-pyridyl-triazole

moiety possesses interesting properties as ligands for transition metals[21] including nickel,[22] iridium,[23] iron,[24] ruthenium[23b,25] or palladium[12j,26] as representative examples. The corresponding reported complexes display appealing optical, electronical, biological, sensing or catalytic properties to name a few which enable their applications in a wide array of fields. [12j,21-26] As a consequence, compound **6** is expected to combine the chemical and thermal stabilities of the inorganic core, the intrinsic properties of the metal complexes together with a multivalency known to bring additional properties in different domains (catalysis,[12j] biology,[13k]).

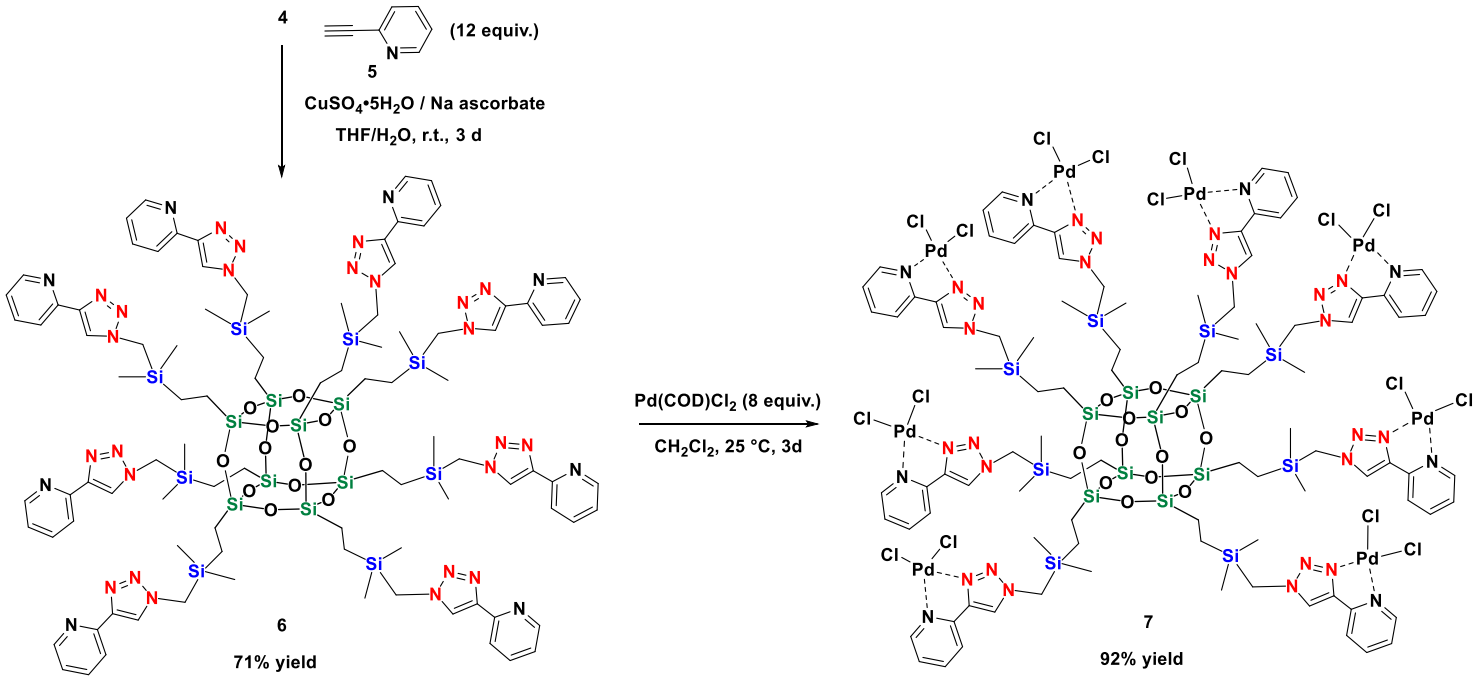

Scheme 3. Preparation of the octa(2-pyridyl-triazole) ligand **6** *via* CuAAC and its complexation with $Pd(COD)Cl_2$ to afford the corresponding octa-palladium complex **7**.

Subsequently, compound **6** was allowed to react with $Pd(COD)Cl_2$ (1 equiv of Pd per *N,N*-pincer) to afford the octa-palladium complex **7** in 92% yield (Scheme 3). The latter could be solubilized in deuterated DMSO and analyzed by multinuclear NMRs. As expected, two singlets were observed on the ^{29}Si NMR spectrum, one for T-group silicon atoms at -61.40 ppm and the other one at 5.92 ppm corresponding to the carbosilane moiety (Figure S13). The ^{1}H NMR

spectrum clearly highlighted the impact of the coordination to palladium on chemical shifts of the triazole and pyridinic protons, leading to a general downfield movement in the position of their ^{1}H resonances (Figure S11). The most impacted signal corresponds to the singlet of the triazolic proton that shifted from 8.38 ppm in ligand **6** to 9.04 ppm in the corresponding palladium complex **7**, which is consistent with data reported for related 2-pyridyl-triazole palladium(II) complexes.[26] The ^{13}C NMR spectrum was in accordance with a successful coordination of Pd on the eight *N,N*-pincers present on the T_8 cage (Figure S12). The elemental analysis was also consistent with the presence of eight palladium atoms per molecule.

It is worthy to note that ligand **6** bearing eight *N,N*-pincers appears as complementary to previously reported POSS functionalized by 2-pyridyl-triazole moieties, namely the monosubstituted dichloro-(3-(1H-1,2,3-triazol-4-yl-2-pyridine)propyl)hepta(i-butyl)octasilsesquioxane (Scheme 4, a) and the deca-substituted deca(3-(1H-1,2,3-triazol-4-yl-2-pyridine)propyl)decasilsesquioxane (Scheme 4, b).[12j] In the former case (T_8 cage with one *N,N*-pincer), the corresponding palladium complex could be obtained successfully in the presence of $Pd(COD)Cl_2$ (Scheme 4, a, **T_8-Pd$_1$**). In the latter case (T_{10} cage with ten *N,N*-pincers), the coordination to Pd(II) was not complete and leads to an insoluble compound bearing 4.6 Pd(II) ions per T_{10} cage (Scheme 4, b, **T_{10}-Pd$_{4.6}$**). Both of these complexes were investigated as catalysts for Suzuki-Miyaura couplings and found to display similar activities.[12j] Interestingly, insoluble **T_{10}-Pd$_{4.6}$** could be reused 5 consecutive times with no loss of activity contrary to its soluble monomeric counterpart **T_8-Pd$_1$**.

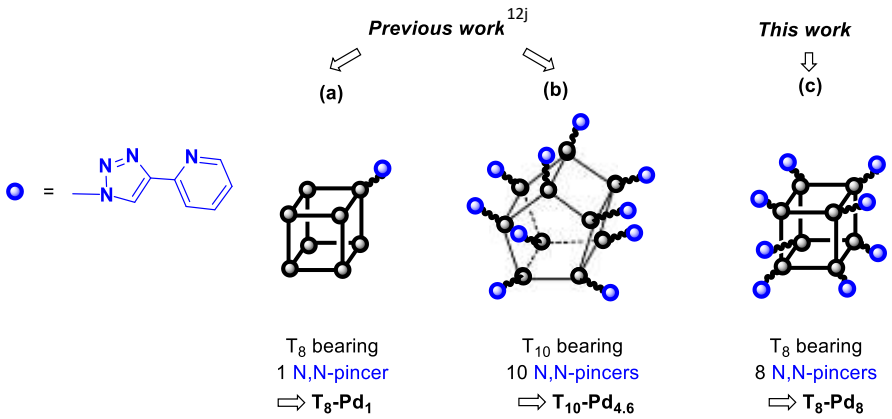

Scheme 4. Previously reported T_8 and T_{10} cages bearing one or ten 2-pyridyl-triazole moieties (*N,N*-pincers) respectively and their corresponding palladium complexes; comparison with the structure of the complex reported in this work.

The performances of related Pd(II) complex **7** reported here were next evaluated in the same model reaction as **T_8-Pd$_1$** and **T_{10}-Pd$_{4.6}$**. Therefore, 4-bromoanisole **8** was allowed to react with phenylboronic acid **9** in the presence of **7** (1.4 mol% Pd) and potassium carbonate (1 equiv) in an ethanol/water (1:1) mixture. Under these conditions, complex **7** was not soluble (Figure 5). After 4h at 60 °C and washing the solid twice with degassed ethanol under argon, the soluble part of the reaction mixture was analyzed by ^{1}H NMR using mesitylene as the standard. The expected biaryl compound **10** was obtained in 98% yield (TON = 71). Reactants **8**, **9**, K_2CO_3 and solvents were next added and the next cycle achieved. Using this procedure, catalyst **7** could be used four times with no loss of activity. Overall, the performances of **7** were found to be comparable to those reported for the related **T_{10}-Pd$_{4.6}$** complex both in terms of activity (98% yield of **10** corresponding to a TON of 71 for **7** versus 93% yield of **10** corresponding to a TON of 66 for **T_{10}-Pd$_{4.6}$**) and recyclability (4 consecutive runs with no loss of activity for **7** versus 5 for **T_{10}-Pd$_{4.6}$**). In our case, the decrease of activity observed for the fifth cycle was likely due to a loss of the catalyst during the recovery by removing the supernatant via cannulation. Indeed, around 5% of the mass of the

catalyst was lost during each recycling experiment. For cycles 2 to 4, this loss did not prevent the full conversion of 4-bromoanisole thus showing that **7** is active even for Pd loading lower than 1.4 mol%. However, for the fifth cycle, there was obviously no Pd enough to promote the Suzuki coupling quantitatively. It is worthy to note that no obvious change in the structure of the catalyst could be found after 5 cycles according to ^{1}H NMR. Lastly, although the TONs obtained for POSS-based recyclable catalysts **T$_{10}$-Pd$_{4.6}$** and **7** are not outstanding as compared to the best systems reported for Suzuki-couplings, the temperature conditions are mild (60 °C) and the solvent eco-compatible.

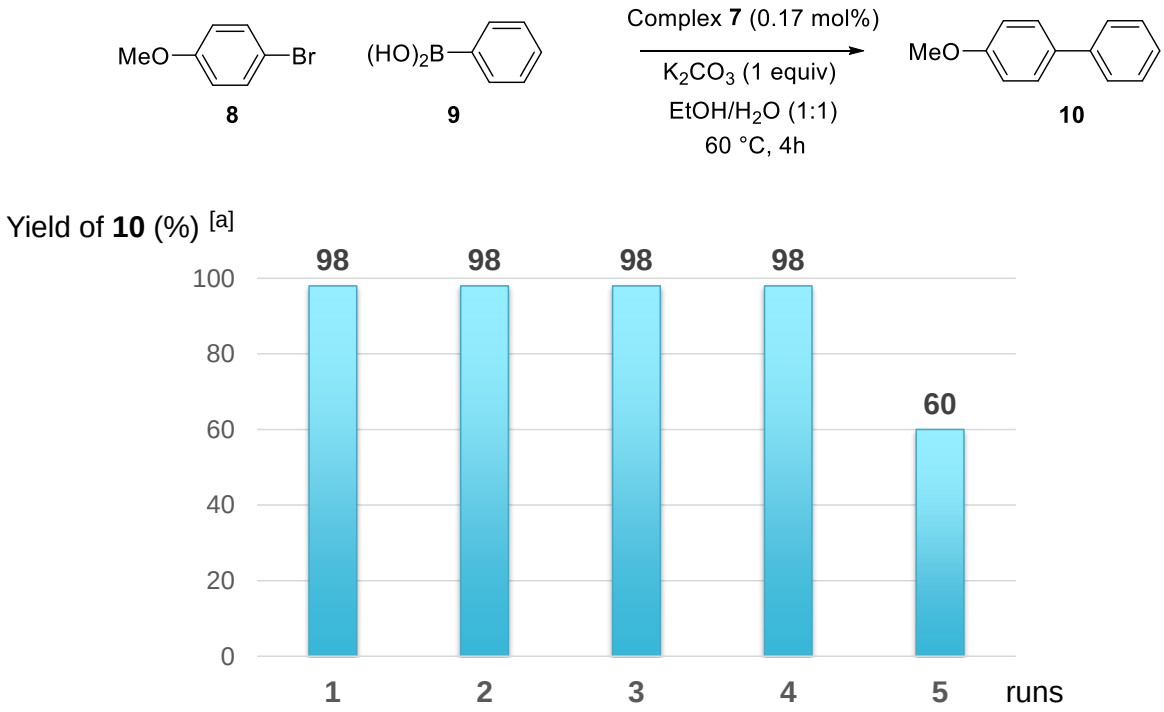

Figure 5. Catalytic performances of **7** (1.4 mol% Pd) in the Suzuki-Miyaura coupling of 4-bromoanisole **8** and phenylboronic acid **9** and its recycling abilities. [a] **7** (0.53 µmol), **8** (0.3 mmol), **9** (0.33 mmol), K_2CO_3 (0.3 mmol), EtOH/H_2O (1:1, 2.4 mL). Yields determined according to ^{1}H NMR spectra using mesitylene as standard. Selectivity 100%.

It is noteworthy that the catalytically active and recyclable complex **7** can be prepared in high yield (57% over 4 steps from the commercially available POSS **1**) and that this multi-step preparation only requires one column chromatography aiming at removing copper used in the CuAAC (Scheme 3).

Conclusion

In summary, a convenient, high-yielding and scalable synthetic pathway to unprecedented chloro- (**3**) and azido (**4**) functionalized T_8 cages have been described. The former (**3**) can be obtained through perfectly regioselective hydrosilylation of octavinylsilsesquioxane with chloromethyldimethylsilane (92% yield), while **4** is quantitatively prepared from **3** in the presence of sodium azide without cage rearrangement (95% yield). Both **3** and **4** are readily purified and no column chromatography is needed. **4** was next shown to undergo copper-catalyzed azide-alkyne [3+2] cycloaddition with 2-ethynylpyridine, a challenging alkyne substrate, to give rise to a multidentate ligand bearing eight 2-pyridyl-triazole moieties. The coordination of the eight *N,N*-pincers to palladium (II) yielded the corresponding octa-palladium complex able to quantitatively promote the coupling of anisole and phenylboronic acid. The low solubility of this catalytic complex in the reaction medium enabled its recovery and recycling with four cycles being achieved with no loss of activity. Further applications of these readily prepared T_8 cages are currently underway in our laboratory.

EXPERIMENTAL SECTION.

All reactions were performed under an argon atmosphere unless otherwise noted. Diethyl ether, toluene, THF and DMF were dried using mBRAUN purification system. Triethylamine was distilled from potassium hydroxide, stored on potassium hydroxide under an argon atmosphere with protection from light, dichloromethane was distilled from calcium hydride, stored on activated 4Å molecular sieves under an argon atmosphere. (Chloromethyl)dimethylsilane and

Karstedt's catalyst (in xylene, 2% Pt) were purchased from Sigma-Aldrich, octavinyloctasilsesquioxane, sodium azide, sodium ascorbate, 2-ethynylpyridine, phenylboronic acid and 4-bromoanisole were purchased from Tokyo Chemical Industry Co., Ltd., copper(II) sulfate pentahydrate, sodium iodide and dichloro(η-cycloocto-1,5-diene)palladium(II) were purchased from FUJIFILM Wako Pure Chemical Co. Chemical Reagents and all of these reagents were used as received, without further purification.

The Fourier transformation nuclear magnetic resonance (NMR) spectra were obtained using a JEOL JNM-ECA 600 (^{1}H at 600.17 MHz, ^{13}C at 150.91 MHz, ^{29}Si at 119.24 MHz) NMR instruments. For ^{1}H NMR, chemical shifts are reported as δ units (ppm) relative to $SiMe_4$ (TMS) and the residual solvent peaks were used as standards. For ^{13}C NMR and ^{29}Si NMR, chemical shifts are reported as δ units (ppm) relative to $SiMe_4$ (TMS), the residual solvent peaks were used as standards and spectra were obtained with complete proton decoupling. MALDI-TOF mass analysis was carried out with a Shimadzu AXIMA Performance instrument using 2,5-dihydroxybenzoic acid (dithranol) as the matrix and $AgNO_3$ as the ion source. All reagents used were of analytical grade. Elemental analyses were performed at the Center for Material Research by Instrumental Analysis (CIA), Gunma University, Japan. IR spectra were measured using a Shimadzu FTIR-8400S instrument. TGA was carried out under a nitrogen flow (250 mL min^{-1}) or air flow (300 mL min^{-1}) with a heating rate of 10 °C min^{-1} . All samples were measured with temperatures ranging from 50 to 1000 °C, where they remained for 5 min. The weight loss and heating rate were continuously recorded along the experiment.

Synthesis of 3

After standard cycles of evacuation and backfilling with dry and pure argon, an oven-dried Schlenk flask equipped with a magnetic stirring bar was charged with octavinyloctasilsesquioxane **1** (1.266 g, 2.0 mmol), dry toluene (24 mL) and chloromethyl(dimethyl)silane (2.92 mL, 24 mmol). And then Karstedt's catalyst [2 x 10^{-3} mmol [Pt] , 46 μL from a commercial bottle (2% platinum in xylene)] was added at room temperature under argon. After the addition, the reaction mixture was allowed to be heated to 40 ˚C and stir for 3 days at 40 ˚C. The reaction mixture was cooled down to room temperature and then passed through a silica plug which was washed twice with dichloromethane. The gathered eluate was evaporated under vacuum to afford the pure product as a white solid **3** (2.76 g, 92%) without any further purification.

^{1}H NMR (600.17 MHz, $CDCl_3$): δ = 0.11 (s, 48H), 0.56-0.59 (m, 16H), 0.68-0.71 (m, 16H), 2.80 (s, 16H) ppm.
$^{13}C\{^{1}H\}$ NMR (150.91 MHz, $CDCl_3$): δ = -4.91, 4.30, 5.18, 30.08 ppm.
$^{29}Si\{^{1}H\}$ NMR (119.24 MHz, $CDCl_3$): δ = 5.38, -66.49 ppm.
MALDI-TOF MS (m/z): 1524.92 ($[M+Na]^+$, calcd 1525.15).
Elemental analysis: Calcd for $C_{40}H_{96}Cl_8O_{12}Si_{16}\cdot H_2O$: C, 31.60; H, 6.50. Found: C, 30.36; H, 6.48.

Synthesis of 4

After standard cycles of evacuation and backfilling with dry and pure argon, an oven-dried three necked flask equipped with a magnetic stirring bar and a condenser was charged with **3** (0.75 g, 0.5 mmol), sodium iodide (75 mg, 0.5 mmol) and sodium azide (0.78 g, 12.0 mmol). Anhydrous THF (28.5 mL) and anhydrous DMF (73 mL) were then added into the mixture at room temperature under argon with vigorous stirring. The reaction mixture was allowed to be heated to 60 ˚C and to stir for 24 h at 60 ˚C. The reaction mixture was cooled down to room temperature, dichloromethane (100 mL) was slowly added and the mixture was stirred for about 10 minutes. And then ice was added into the mixture which was stirred for additional 30 minutes. The organic layer was then washed twice with brine, dried over anhydrous sodium sulfate and evaporated on the rotavapor (with dichloromethane several times to remove traces of DMF) to afford the desired product as a yellowish solid **4** (0.74 g, 95%) without any further purification. The product was recrystallized in THF and methanol to give colorless crystals.

^{1}H NMR (600.17 MHz, $CDCl_3$): δ = 0.10 (s, 48H), 0.56-0.59 (m, 16H), 0.65-0.68 (m, 16H), 2.80 (s, 16H) ppm.
$^{13}C\{^{1}H\}$ NMR (150.91 MHz, $CDCl_3$): δ = -4.58, 4.31, 5.67, 40.71 ppm.
$^{29}Si\{^{1}H\}$ NMR (119.24 MHz, $CDCl_3$): δ = 5.18, -66.59 ppm.
MALDI-TOF MS (m/z): 1431.00 ($[M+Na-5N_2+5H]^+$, calcd 1437.64), 1447.03 ($[M+K-5N_2+5H]^+$, calcd 1453.75).
Elemental analysis: Calcd for $C_{40}H_{96}N_{24}O_{12}Si_{16}\cdot 2H_2O$: C, 30.20; H, 6.34; N, 21.13. Found: C, 28.97; H, 6.31; N, 21.05.

Synthesis of 6

After standard cycles of evacuation and backfilling with dry and pure argon, an oven-dried Schlenk flask equipped with a magnetic stirring bar was charged with **4** (0.78 g, 0.5 mmol), 2-

ethynylpyridine (0.61 mL, 6.0 mmol) and dry THF (32 mL). To this solution mixture, 100 μL of copper sulfate pentahydrate degassed aqueous solution (125 mg/mL, 0.05 mmol) and sodium ascorbate (50 mg, 0.25 mmol) were added under argon. The solution was allowed to stir at 25 ˚C for 1 days. Additional 100 μL of copper sulfate pentahydrate degassed aqueous solution (125 mg/mL, 0.05 mmol) and sodium ascorbate (50 mg, 0.25 mmol) were added under argon into the reaction mixture which was allowed to stir for additional 1 day at 25 ˚C. Additional 100 μL of copper sulfate pentahydrate degassed aqueous solution (125 mg/mL, 0.05 mmol) and sodium ascorbate (50 mg, 0.25 mmol) were added under argon into the reaction mixture which was allowed to stir for additional 1 day at 25 ˚C. And then water was added into the reaction mixture which was extracted 3 times with dichloromethane. The collected organic layer was washed with brine (x 3) and dried over anhydrous sodium sulfate. The solvents were evaporated on the rotavapor to give a crude product which was dried under vacuum at 100 ˚C for 3 hours (to remove the excess of 2-ethylnylpyridine). And then the crude product was purified by column chromatography to remove copper (eluent: CH_2Cl_2/MeOH = 10/1) to afford a desired product **6** as a pale yellow solid (0.84 g, 71%).

^{1}H NMR (600.17 MHz, $CDCl_3$): δ = 0.11 (s, 48H), 0.61-0.64 (m, 16H), 0.75-0.77 (m, 16H), 3.99 (s, 16H), 7.18 (dd, *J* = 7.8 Hz, 4.8 Hz, 8H), 7.73 (td, *J* = 7.8 Hz, 1.8 Hz, 8H), 8.10 (s, 8H), 8.12 (d, *J* = 7.8 Hz, 8H), 8.52 (d, *J* = 4.8 Hz, 8H) ppm.
^{1}H NMR (600.17 MHz, DMSO-d_6): δ = 0.004 (s, 48H), 0.56-0.65 (m, 32H), 4.07 (s, 16H), 7.27 (dd, *J* = 7.8 Hz, 4.8 Hz, 8H), 7.81 (td, *J* = 7.8 Hz, 7.8 Hz, 1.8 Hz, 8H), 7.97 (d, *J* = 7.8 Hz, 8H), 8.38 (s, 8H), 8.53 (dd, *J* = 4.8 Hz, 1.8 Hz, 8H) ppm.
^{13}C{^{1}H} NMR (150.91 MHz, $CDCl_3$): δ = -4.40, 4.29, 5.88, 40.82, 120.38, 122.87, 123.34, 137.50, 147.61, 148.93, 150.33 ppm.
^{29}Si{^{1}H} NMR (119.24 MHz, $CDCl_3$): δ = 4.86, -66.72 ppm.
MALDI-TOF MS (m/z): 2381.05 ($[M+H]^+$, calcd 2380.72), 2403.05 ($[M+Na]^+$, calcd 2402.71).

Synthesis of 7

After standard cycles of evacuation and backfilling with dry and pure argon, a Schlenk flask equipped with a magnetic stirring bar was charged with **6** (70 mg, 0.0294 mmol), Pd(COD)Cl_2 (67 mg, 0.2353 mmol) and distilled dichloromethane (6.5 mL). The mixture was allowed to stir at 25 ˚C for 3 days. After 3 days, the reaction mixture was filtered and washed with dichloromethane to afford an orange solid **7** (dried under vacuum at 60 ˚C, 103 mg, yield 92%).

^{1}H NMR (600.17 MHz, DMSO-d_6): δ = 0.10 (s, 48H), 0.66-0.72 (m, 32H), 4.31 (s, 16H), 7.56-7.59 (m, 8H), 8.18-8.24 (m, 16H), 8.79 (d, *J* = 5.84 Hz, 8H), 9.04 (s, 8H) ppm.

$^{13}C\{^1H\}$ NMR (150.91 MHz, DMSO-d_6): δ = -4.61, 3.64, 5.20, 42.73, 122.33, 125.33, 126.30, 141.23, 147.06, 148.25, 149.24 ppm.
$^{29}Si\{^1H\}$ NMR (119.24 MHz, DMSO-d_6): δ = 5.92, -61.40 ppm.
Elemental analysis: Calcd for $C_{96}H_{136}N_{32}O_{12}Pd_8Si_{16}\cdot 5H_2O$: C, 29.65; H, 3.78; N, 11.53. Found: C, 28.73; H, 3.84; N, 11.40.

Experimental procedure for the catalytic recycling experiments (Suzuki-Miyaura cross-coupling reaction)

After standard cycles of evacuation and backfilling with dry and pure argon, a Schlenk flask equipped with a magnetic stirring bar was charged with **7** (2 mg, 0.0042 mmol of Pd) and degassed EtOH/H_2O (1/1, 2.4 mL). 4-bromoanisole (38 μL, 0.3 mmol), phenylboronic acid (40 mg, 0.33 mmol) and K_2CO_3 (41 mg, 0.3 mmol) were added into the Schlenk under argon. The mixture was heated to 60 ˚C and allow to stir for 4 h at 60 ˚C. After 4 h, the reaction mixture was cooled down to room temperature, water (1 mL) and ethyl acetate (2 mL) were added. The mixture was extracted with ethyl acetate (x 2), the gathered organic layer was dried over anhydrous Na_2SO_4 and evaporated on the rotavapor at room temperature. Mesitylene (14 uL, 0.1 mmol) used as standard was added into the crude product, ^1H NMR analysis (in $CDCl_3$) was performed to estimate the yield of coupling product.

For recycling experiment, after the reaction, the catalyst stayed insoluble and in the bottom of the Schlenk flask. The mixture (upper layer) was taken up via cannulation under argon and a small amount of degassed EtOH was added into Schlenk to wash (x 2), and then degassed EtOH/H_2O (1/1, 2.4 mL), 4-bromoanisole (38 uL, 0.3 mmol), phenylboronic acid (40 mg, 0.33 mmol) and K_2CO_3 (41 mg, 0.3 mmol) were added into the Schlenk under argon to perform the new cycle of reaction.

Crystallography. For crystal data, data collection, and refinement, see ESI, CCDC-2059283 for **4** contain the supplementary crystallographic data for this paper.

ASSOCIATED CONTENT

Supporting Information: ^1H, ^{13}C, ^{29}Si NMR spectra for compounds **3, 4, 6** and **7**, MALDI-TOF MS spectra and IR spectra for **3**, **4** and **6**, thermal properties (TGA) for **3** and **4**, crystallographic data for **4**. The Supporting Information is available free of charge on the ACS Publications website.

AUTHOR INFORMATION

Corresponding Authors

Masafumi Unno. Department of Chemistry and Chemical Biology, Graduate School of Science and Technology, Gunma University, Kiryu 376-8515, Gunma, Japan; orcid.org/0000-0003-2158-1644; Email: unno@gunma-u.ac.jp
Armelle Ouali. Institut Charles Gerhardt Montpellier ICGM, Univ. Montpellier, CNRS, ENSCM, Montpellier 34090, France; orcid.org/0000-0001-7436-776X. Email: armelle.ouali@enscm.fr.

Authors

Yujia Liu. Gunma University Initiative for Advanced Research (GIAR)-International Open Laboratory with Institute Charles Gerhardt Montpellier (UMR5253 CNRS-UM-ENSCM), France. Gunma University, Kiryu 376-8515, Japan. Department of Chemistry and Chemical Biology, Graduate School of Science and Technology. Gunma University, Kiryu 376-8515, Japan.
Institut Charles Gerhardt Montpellier ICGM, Univ. Montpellier, CNRS, ENSCM, Montpellier 34090, France; orcid.org/0000-0001-7436-776X. Email: armelle.ouali@enscm.fr.

Nobuhiro Takeda. Department of Chemistry and Chemical Biology, Graduate School of Science and Technology. Gunma University, Kiryu 376-8515, Japan.
Kyoka Koizumi. Department of Chemistry and Chemical Biology, Graduate School of Science and Technology. Gunma University, Kiryu 376-8515, Japan.

Author Contributions

Conceptualization: Armelle Ouali, Yujia Liu, Masafumi Unno; Methodology : Armelle Ouali, Yujia Liu; Formal analysis and investigation : Yujia Liu, Kyoka Koizumi, Nobuhiro Takeda; Writing – original draft preparation: Armelle Ouali, Yujia Liu; Writing – review and editing: Armelle Ouali, Masafumi Unno, Yujia Liu; Funding acquisition: Masafumi Unno, Armelle Ouali. All authors have read and agreed to the published version of the manuscript.

ACKNOWLEDGMENT

The authors acknowledge the Gunma University Initiative for Advanced Research (GIAR) for funding the Open International Laboratory and the grant to Y. L, CNRS and New Energy and Industrial Technology Development Organization (NEDO) for funding, and JASSO for K. K. travel grants to Montpellier.

Notes

The authors declare no competing financial interest.

REFERENCES

(1) (a) Laine, R. M.; Roll, M. F. Polyhedral Phenylsilsesquioxanes. *Macromolecules* **2011**, *44*, 1073-1109; (b) Cordes, D. B.; Lickiss, P. D.; Rataboul, F. Recent Developments in the Chemistry of Cubic Polyhedral Oligosilsesquioxanes. *Chem. Rev*. **2010**, *110*, 2081-2173; (c) Cordes, D. B.; Lickiss, P. D. in *Applications of Polyhedral Oligomeric Silsesquioxanes, Advances in Silicon Science 3*, ed. Hartmann-Thompson, C. Springer, **2011**; (d) Du, Y.; Liu, H. Cage-like silsesquioxanes-based hybrid materials. *Dalton Trans.*, **2020**, *49*, 5396-5405.

(2) Chen, F. ; Liu, F. ; Zhang, Q. ; Cai, R. ; Wu, Y. ; Ma, X. Polyhedral Oligomeric Silsesquioxane Hybrid Polymers: Well-Defined Architectural Design and Potential Functional Applications. *Macromol. Rapid Commun*. **2019**, *40*, 1900101.

(3) Zhou, H.; Ye, Q.; Xu, J. Polyhedral oligomeric silsesquioxane-based hybrid materials and their applications. *Mater. Chem. Front.*, **2017**, *1*, 212-230.

(4) Calabrese, C.; Aprile, C.; Gruttadauria, M.; Giacalone, F. POSS nanostructures in catalysis. *Catal. Sci. Technol.*, **2020**, *10*, 7415-7447.

(5) (a) Kunthom, R.; Piyanuch, P.; Wanichacheva, N.; Ervithayasuporn, V. Cage-like silsesquioxanes bearing rhodamines as fluorescence Hg^{2+} sensors. *J. Photochem. Photobiol. A* **2018**, *356*, 248–255; (b) Chanmungkalakul, S.; Ervithayasuporn, V.; Hanprasit, S.; Masik, M.; Prigyai, N.; Kiatkamjornwong, S. Silsesquioxane cages as fluoride sensors. *Chem. Commun*. **2017**, *53*, 12108-12111.

(6) Chen, X. ; Dumée, L. F. Polyhedral Oligomeric Silsesquioxanes (POSS) Nano-Composite Separation Membranes – A Review. *Adv. Eng. Mater.* **2019**, *21*, 1800667.

(7) (a) Dudziec, B. ; Zak, P. ; Marciniec, B. Synthetic Routes to Silsesquioxane-Based Systems as Photoactive Materials and Their Precursors. *Polymers*, **2019**, *11*, 504; (b) Chan, K. L.; Sonar, P.; Sellinger, A. Cubic silsesquioxanes for use in solution processable organic light emitting diodes (OLED). *J. Mater. Chem.*, **2009**, *19*, 9103-9120.

(8) Wang, J. ; Du, W. ; Zhang, Z. ; Gao, W. ; Li, Z. Biomass/polyhedral oligomeric silsesquioxane nanocomposites : Advances in preparation strategies and performances. *J. Appl. Polym. Sci.*, **2021**, *138*, e49641.

(9) (a) Huisgen, R. Kinetics and reaction mechanisms: selected examples from the experience of forty years. *Pure & Appl. Chem.*, **1989**, *61*, 613-628; (b) Xi, W.; Scott, T. F.; Kloxin, C. J.; Bowman, C. N. Click Chemistry in Materials Science. *Adv. Funct. Mater.* **2014**, *24*, 2572-2590.

(10) Liu, Y.; Kigure, M.; Koizumi, K.; Takeda, N.; Unno, M.; Ouali, A. Synthesis of Tetrachloro, Tetraiodo, and Tetraazido Double-Decker Siloxanes. *Inorg. Chem.* **2020**, *59*, 15478-15486.

(11) For D_2T_8 DDSQ bearing two azido functions: (a) Ervithayasuporn, V.; Wang, X.; Kawakami, Y. Synthesis and Characterization of Highly Pure Azido-Functionalized Polyhedral Oligomeric Silsesquioxanes (POSS). *Chem. Commun.*, **2009**, 5130-5132; (b) Wei, K.; Wang, L.; Zheng, S. Organic-Inorganic Copolymers with Double-Decker Silsesquioxane in the Main Chains by Polymerization via Click Chemistry. *J. Polym. Sci. A Polym. Chem.* **2013**, *51*, 4221-4232; (c) Rzonsowska, M.; Kozakiewicz, K.; Mitula, K.; Duszczak, J.; Kubicki, M.; Dudziec, B. Synthesis of Silsesquioxanes with Substituted Triazole Ring Functionalities and Their Coordination Ability. *Molecules*, **2021**, *26*, 439.

(12) *Applications in polymeric materials:* (a) Chang, P.; Xu, S.; Zhao, B.; Zheng, S. A Design of Shape Memory Networks of Poly(ε-caprolactone)s via POSS-POSS interactions. *Polym. Adv. Technol.* **2019**, *30*, 713-725; (b) Su, Z.; Hsu, C.-H.; Gong, Z.; Feng, X.; Huang, J.; Zhang, R.; Wang, Y.; Mao, J.; Wesdemiotis, C.; Li, T.; Seifert, S.; Zhang, W.; Aida, T.; Huang, M.; Cheng, S. Z. D. Identification of a Frank-Kasper Z Phase from Shape Amphiphile Self-Assembly. *Nature Chem*. **2019**, *11*, 899-905; (c) Li, L.; Zhang, C.; Zheng, S. Synthesis of POSS-Terminated Polycyclooctadiene Telechelics via Ring-Opening Metathesis Polymerization. *J. Polym. Sci. A Polym. Chem.* **2017**, *55*, 223-233; (d) Zheng, Y.; Wang, L.; Zheng, S. Synthesis and Characterization of Heptaphenyl Polyhedral Oligomeric Silsesquioxane-Capped Poly(N-isopropylacrylamide)s. *Eur. Polym. J.*, **2012**, *48*, 945-955; (e) Wang, L.; Zheng, S. Surface Morphology and Dewettability of Self-Organized Thermosets Involving Epoxy and POSS-Capped Poly(ethylene oxide) Telechelics. *Mater. Chem. Phys.* **2012**, *136*, 744-754; (f) Jiang, Z.-Y.; Zhou, Y.; Huang, F.-R.; Du, L. Characterization of a Modified Silicon-Containing Arylacetylene Resin With POSS Functionality. *Chin. J. Polym. Sci.* **2011**, *29*, 726-731; (g) Binder, W. H.; Petraru, L.; Sachenshofer, R.; Zirbs, R. Synthesis of Surface-Modified Nanoparticles via Cycloaddition-Reactions. *Monatshefte für Chemie* **2006**, *137*, 835-841. *Applications in catalysis:* (h) Zhou, Y.; Yang, G.; Lu, C.; Nie, J.; Chen, Z.; Ren, J. POSS Supported C2-symmetric Bisprolinamide as a Recyclable Chiral Catalyst for Asymmetric Aldol reaction. *Catal. Commun.* **2016**,

75, 23-27; (i) Zheng, W.; Lu, C.; Yang, G.; Chen, Z.; Nie, J. POSS Supported Diarylprolinol Silyl Ether as an Efficient and Recyclable Organocatalyst for Asymmetric Michael Addition Reactions. *Catal. Commun*. **2015**, *62*, 34-38; (j) Ervithayasuporn, V.; Kwanplod, K.; Boonmak, J.; Youngme, S.; Sangtrirutnugul, P. Homogeneous and Heterogeneous Catalysts of Organopalladium Functionalized-Polyhedral Oligomeric Silsesquioxanes for Suzuki-Miyaura Reaction. *J. Catal*. **2015**, *332*, 62-69.

(13) *Applications in polymeric materials:* (a) Ozdogan, R.; Daglar, O.; Durmaz, H.; Tasdelen, M. A. Aliphatic Polyester/polyhedral Oligomeric Silsesquioxanes Hybrid Networks via Copper-free 1,3-dipolar Cycloaddition Click Reaction. *J. Polym. Sci. A Polym. Chem.* **2019**, *57*, 2222-2227; (b) Zhang, J.; Si, D.; Wang, S.; Liu, H.; Chen, X.; Zhou, H.; Yang, M.; Zhang, G. Novel Organic/Inorganic Hybrid Star Polymer Surface-Crosslinked with Polyhedral Oligomeric Silsesquioxane. *Macromol. Res.* **2019**, DOI 10.1007/s13233-020-8021-4; (c) Doganci, M. D.; Aynali, F.; Doganci, E.; Ozkoc, G. Mechanical, Thermal and Morphological Properties of Poly(lactic acid) by Using Star-Shaped Poly(ε-caprolactone) with POSS core. *Eur. Polym. J.* **2019**, *121*, 109316; (d) Uner, A.; Doganci, E.; Tasdelen, M. A. Non-Covalent Interactions of Pyrene End-Labeled Star Poly(ε-caprolactone)s with Fullerene. *J. Appl. Polym. Sci.* **2018**, *135*, 46520; (e) Namvari, M.; Du, L.; Stadler, F. J. Graphene Oxide-Based Silsesquioxane-Crosslinked Networks - Synthesis and Rheological Behavior. *RSC Adv.*, **2017**, *7*, 21531-21540; (f) Ziarani, G. M.; Nahad, M. S.; Lashgari, N.; Badiei, A. Synthesis of a Nanostructured Composite: Octakis(1-propyl-1*H*-1,2,3-triazole-4-yl(methyl-2-chlorobenzoate)octasilsesquioxane via Click Reaction. *Acta Chim. Slov.* **2015**, *62*, 709-715; (g) Li, Y.; Wan, L.; Huang, F.; Du, L. Core-Shell Octa(azidopropyl) POSS-PEO Micelle via "Click" Chemistry. *J. Mol. Liq.* **2014**, *196*, 238-243; (h) Yuan, W.; Liu, X.; Zou, H.; Li, J.; Yuan, H.; Ren, J. Synthesis, Self-Assembly, and Properties of Homoarm and Heteroarm Star-Shaped Inorganic-Organic Hybrid Polymers with a POSS Core. *Macromol. Chem. Phys.* **2013**, *214*, 1580-1589; (i) Yuan, W.; Liu, X.; Zou, H.; Ren, J. Environment-Induced Nanostructural Dynamical-Change Based On Supramolecular Self-Assembly of Cyclodextrin and Star-Shaped Poly(ethylene oxide) with Polyhedral Oligomeric Silsesquioxane Core. *Polymer* **2013**, *54*, 5374-5381; (j) Ge, Z.; Wang, D.; Zhou, Y.; Liu, H.; Liu, S. Synthesis of Organic/Inorganic Hybrid Quatrefoil-Shaped Star-Cyclic Polymer Containing a Polyhedral Oligomeric Silsesquioxane Core. *Macromolecules* **2009**, *42*, 2903-2910; *Biological applications:* (k) Rahimifard, M.; Ziarani, G. M.; Badiei, A.; Yazdian, F. Synthesis of Polyhedral Oligomeric Silsesquioxane (POSS) with Multifunctional Sulfonamide Groups Through Click Chemistry. *J. Inorg. Organomet. Polym.* **2017**, *27*, 1037-1044; (l) Pérez-Ojeda, M. E.; Trastoy, B.; Rol, Á. ; Chiara, M. D.; García-Moreno, I. ; Chiara, J. L. Controlled Click-Assembly of Well-Defined Hetero-Bifunctional Cubic Silsesquioxanes and Their Application in Targeted Bioimaging. *Chem. Eur. J.* **2013**, *19*, 6630-6640. (m) Trastoy, B.; Bonsor, D. A.; Pérez-Ojeda, M. E.; Jimeno, M. L.; Méndez-Ardoy, A.; García Fernández, J. M.; Sundberg, E. J.; Chiara, J. L. Synthesis and Biophysical Study of Disassembling Nanohybrid Bioconjugates with a Cubic Octasilsesquioxane Core. *Adv. Funct. Mater*. **2012**, *22*, 3191-3201; (n) Fabritz, S.; Heyl, D.; Bagutski, V.; Empting, M.; Rikowski, E.; Frauendorf, H.; Balog, I.; Fessner, W.-D.; Schneider, J. J.; Avrutina, O.; Kolmar, H. Towards Click Bioconjugations on Cube-Octameric Silsesquioxane Scaffolds. *Org. Biomol. Chem.*, **2010**, *8*, 2212-2218; (o) Heyl, D.; Rikowski, E.; Hoffmann, R. C.; Schneider, J. J.; Fessner, W.-D. A "Clickable" Hybrid Nanocluster of Cubic Symmetry. *Chem. Eur. J.* **2010**, *16*, 5544-5548. *Optoelectronic applications:* (p) Pérez-Ojeda, M. E.; Trastoy, B.; López-Arbeloa, Í.; Bañuelos, J. ; Costela, Á. ; García-Moreno, I. ; Chiara, J. L. Click Assembly of Dye-Functionalized Octasilsesquioxanes for Highly Efficient and Photostable Photonic Systems. *Chem. Eur. J.* **2011**, *17*, 13258-13268. (q) Ak, M.; Gacal, B.; Kiskan, B.; Yagci, Y.; Toppare, L. Enhancing Electrochromic Properties of Polypyrrole by Silsesquioxane Nanocages. *Polymer* **2008**, *49*, 2202-2210.

(14) Trastoy, B. ; Pérez-Ojeda, M. E. ; Sastre, R. ; Chiara, J. L. Octakis(3-azidopropyl)octasilsesquioxane: A Versatile Nanobuilding Block for the Efficient Preparation of Highly Functionalized Cube-Octameric Polyhedral Oligosilsesquioxanes Frameworks Through Click Assembly. *Chem. Eur. J.* **2010**, *16*, 3833-3841.

(15) For applications of azido-decorated T_{10}: (a) Liu, G.; Feng, X.; Lang, K.; Zhang, R.; Guo, D.; Yang, S.; Cheng, S. Z. D. Dynamics of Shape-Persistent Giant Molecules: Zimm-like Melt, Elastic Plateau, and Cooperative Glass-like. *Macromolecules* **2017**, *50*, 6637-6646; (b) Feng, X.; Zhu, S.; Yue, K.; Su, H.; Guo, K.; Wesdemiotis, C.; Zhang, W.-B.; Cheng, S. Z. D.; Li, Y. T_{10} Polyhedral Oligomeric Silsesquioxane-Based Shape Amphiphiles with Diverse Head Functionalities via "Click" Chemistry. *ACS Macro Lett.* **2014**, *3*, 900-905.

(16) Liu, Y.; Onodera, K.; Takeda, N.; Ouali, A.; Unno, M. Synthesis and Characterization of Functionalizable Silsesquioxanes with Ladder-type Structures. *Organometallics* **2019**, *38*, 4373-4376.

(17) Hurkes, N. ; Bruhn, C.; Belaj, F.; Pietschnig, R. Silanetriols as Powerful Starting Materials for Selective Condensation to Bulky POSS Cages. *Organometallics*, **2014**, *33*, 7299-7306.

(18) Dutkiewicz, M. ; Maciejewski, H.; Marciniec, B. Synthesis of Azido-, Hydroxy- and Nitro-, Hydroxy-Functionalized Spherosilicates via Oxirane Ring-Opening Reactions. *Synlett*, **2012**, *44*, 881-884. Recently, the same

epoxy ring-opening reaction to introduce the azido moiety via nucleophilic substitution was also applied to commercially available octakis-glycidyl-POSS.[13a]

(19) For further applications of the spherosilicate-based cubic building block, see for example: (a) Doganci, E.; Tasdelen, M. A.; Yilmaz, F. Synthesis of Miktoarm Star-Shaped Polymers with POSS Core via a Combination of CuAAC Click Chemistry, ATRP, and ROP Techniques. *Macromol. Chem. Phys.*, **2015**, *216*, 1823-1830; (b) Tinmaz, H. B.; Arslan, I.; Tasdelen, M. A. Star Polymers by Photoinduced Copper-Catalyzed Azide-Alkyne Cycloaddition Click Chemistry. *J. Polym. Sci., Part A: Polym. Chem.* **2015**, *53*, 1687-1695.

(20) Sun, N.; Yu, Z.; Yi, H.; Zhu, X.; Jin, L.; Hu, B.; Shen, Z.; Hu, X. Synthesis of a heterogeneous $Cu(OAc)_2$-anchored SBA-15 catalyst and its application in the CuAAC reaction. *New J. Chem.*, **2018**, *42*, 1612-1616.

(21) (a) Xu, X.; Jerca, V. V.; Hoogenboom, R. Self-healing Metallo-Supramolecular Hydrogel Based on Specific Ni^{2+} Coordination Interactions of Poly(ethyleneglycol) with Bistriazole Pyridine Ligands in the Main Chain. *Macromol. Rapid Commun.*, **2020**, *41*, 1900457; (b) Romero, T.; Orenes, R. A.; Espinosa, A.; Tarraga, A.; Molina, P. Synthesis, Structural Characterization, and Electrochemical and Optical Properties of Ferrocene-Triazole-Pyridine Triads. *Inorg. Chem.*, **2011**, *50*, 8214-8224.

(22) Schweinfurth, D.; Su, C.-Y.; Wei, S.-C.; Braunstein, P.; Sarkar, B. Nickel complexes with "click"-derived pyridyl-triazole ligands: weak intermolecular interactions and catalytic ethylene oligomerisation. *Dalton Trans.*, **2012**, *41*, 12984-12990

(23) (a) Juricek, M.; Felici, M.; Contreras-Carballada, P.; Lauko, J.; Rodriguez Bou, S.; Kouwer, P. H. J.; Brouwer, A. M.; Rowan, A. E. Triazole-pyridine ligands: a novel approach to chromophoric iridium arrays. *J. Mater. Chem.*, **2011**, *21*, 2104-2111; (b) Felici, M.; Contreras-Carballada, P.; Vida, Y.; Smits, J. M. M.; Nolte, R. J. M.; De Cola, L.; Williams, R. M.; Feiters, M. C. Ir^{III} and Ru^{II} Complexes Containing Triazole-Pyridine Ligands: Luminescence Enhancement upon Substitution with β-Cyclodextrin. *Chem. Eur. J.*, **2009**, *15*, 13124-13134.

(24) Kobayashi, Y.; Kameda, T.; Hoshino, M.; Fujii. N.; Ohno, H.; Oishi, S. Fe(II)-Complexation of tripodal hexapeptide ligands with three bidentate triazolylpyridines: induction of metal-centred chirality by peptide macrocyclization. *Dalton Trans.*, **2017**, *46*, 13673-13676.

(25) (a) Guven, N.; Sultanova, H.; Ozer, B.; Yucel, B.; Camurlu, P. Tuning of electrochromic properties of electrogenerated polythiophenes through Ru(II) complex tethering and backbone derivatization. *Electrochimica Acta.*, **2020**, *329*, 135134; (b) Kreofsky, N. W.; Dillenburg, M. D.; Villa, E. M.; Fletcher, J. T. Ru(II) coordination compounds of N-N bidentate chelators with 1,2,3 triazole and isoquinoline subunits: synthesis, spectroscopy and antimicrobial properties. *Polyhedron*, **2020**, *177*, 114259; (c) Leckie, L.; Mapolie, S. F. Triazole complexes of ruthenium immobilized on mesoporous silica as recyclable catalysts for octane oxidation. *Catal. Commun.*, **2019**, *131*, 105803; (d) Leckie, L.; Mapolie, S. F. Mesoporous silica as phase transfer agent in the biphasic oxidative cleavage of alkenes using triazole complexes of ruthenium as catalyst precursors. *Appl. Catal. A: Gen.*, **2018**, *565*, 76-86; (e) Chowdhury, B.; Khatua, S.; Dutta, R.; Chakraborty, S.; Ghosh, P. Bis-Heteroleptic Ruthenium(II) Complex of a Triazole Ligand as a Selective Probe for Phosphates. *Inorg. Chem.*, **2014**, *53*, 8061-8070.

(26) Zhang, G.; Wang, Y.; Wen, X.; Ding, C.; Li, Y. Dual-functional click-triazole: a metal chelator and immobilization linker for the construction of a heterogeneous palladium catalyst and its application for the aerobic oxidation of alcohols. *Chem. Commun.*, **2012**, *48*, 2979-2981.

SYNOPSIS

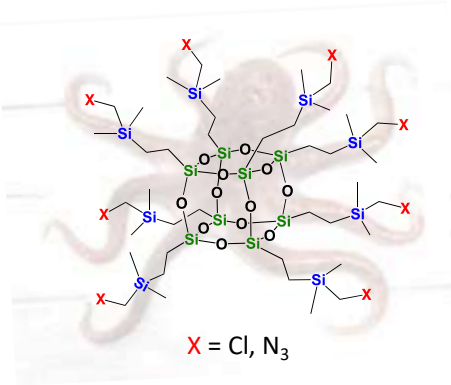

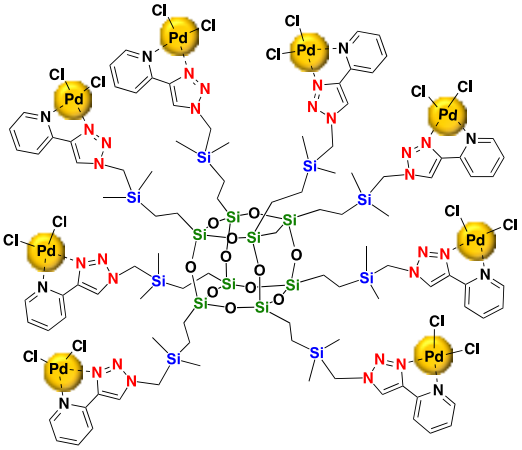

- Fast and scalable preparation
- Excellent yields (> 90%)
- Good selectivity

- Total yield: 57% from commercial octavinylsilsesquioxane
- Catalyst for Suzuki coupling
- Recyclable 4 times without loss of activity